IDENTIFICATION OF MECHANICAL PROPERTIES OF COMPOUND FEEDS FOR MODELLING THE PROCESSES OF THICKENING AND COMPACTION

J. CZABAN, Z. KAMINSKI

Bialystok University of Technology, Poland

Physical relationships for the analysis of stress and strain in modeling of compaction process of materials of vegetable origin with properties of plasticity are described. The study is based on the yield condition formulated by Green. The analysis uses the basic functions of porosity and the Amontons–Coulomb and Prandl laws of friction for porous materials. The experimental and theoretical tests of fodder mixture compression are performed in a closed chamber. The identification of material constants is made by the numerical methods and nonlinear regression equations describing the pressure on the stamps of the chamber.

Keywords: *granular solids, compaction, pressure, yield criterion.*

The aggregation of loose and porous materials by mechanical compaction into a product of a specific shape and dimensions is applied in powder metallurgy [1, 2], ceramic [3, 4], chemical and pharmaceutical [5, 6] industries. Compaction of loose materials of plant origin is used in the food and feed [7] or energy [8, 9] industries. Interestingly, a number of similarities can be noticed in the above-mentioned applications in applied technologies and equipment used for the production of compacted materials. Currently, for determining the optimal parameters of the process of compaction on stamp and rotary presses digital simulation methods are applied, which use mathematical models for loose and porous media regarded as a plastic material. For many years a systematic development of loose material models was taking place, from the Coulomb plasticity model [10], Drucker–Prager [11], Cam-Clay [12], Lade [13] to so call density-reinforcement elliptic plasticity models based on the Huber-Mises yield criterion. Among them, the Green [14], Kuhn and Downey [15], Shima and Oyane [16], Doraivelu [17] or Gurson [18] criteria can be distinguished.

The studies of the authors [19] on the modelling of the processes of pressure agglomeration of compound feeds have indicated wider possibilities of applying the loose material plasticity theory to the modelling of the processes of their agglomeration. The thin cross-section method and the loose material density-reinforcement yield criterion [14] were used in the present study to develop a mathematical model for the distribution of stresses during compaction of the compound feeds in a closed chamber. Similarly to [20], the model equations were subsequently used for determining the material parameters by means of intensification of measured force variations at selected points in the compaction chamber.

The main advantage of the adopted research method is the easiness of determining the variations in the material density being thickened, the ease of measuring the compaction pressure and the straightforward nature of the theoretical relationships describing the axially symmetrical stress state.

Corresponding author: J. CZABAN, e-mail: j.czaban@pb.edu.pl

Basic assumptions and solutions. A schematic of the loose material compaction in a closed chamber is shown in Fig. 1. Due to the axially symmetrical stress state and the uniaxial strain state the cylindrical coordinate system $\{r, \varphi, z\}$ is adopted, whose z axis is directed opposite to the stamp displacement direction and, at the same time, is the axis of the system symmetry. This assumption results from the geometry of the chamber and its non-deformability. The origin of the system is positioned at the chamber bottom. It is assumed that the agglomerated material is homogeneous and exhibits isotropic properties. The isotropy of the material results from the random arrangement of particles in the compound feed, and its homogeneity is due to the uniform distribution of individual components and the small difference in size and shape between them. The material is fed by gravity to the compaction chamber. The analysis of thickening is made for the Green elliptic yield criterion [14], known from the metal powder compaction theory, which is written in the form [21]:

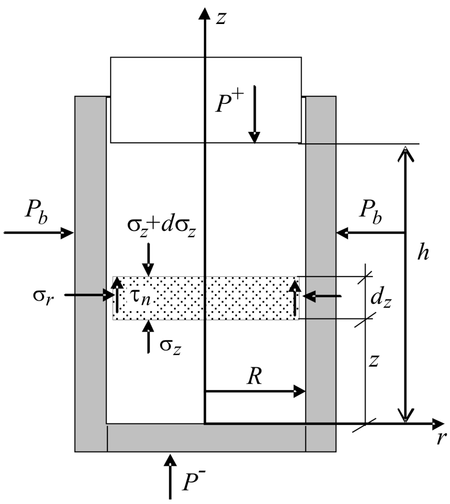

Fig. 1. Schematic of stress action in the closed chamber compaction process.

$$3J_2' + \alpha(\Theta)J_1^2 - \beta(\Theta)\sigma_Y^2 = 0, \qquad (1)$$

where $J_1 = \sigma_z + 2\sigma_r$ is the first invariant of stress tensor, $J_2' = (\sigma_r - \sigma_z)^1/3$ is the second invariant of deviatoric stress tensor, σ_Y is the compressive yield strength, $\alpha(\Theta)$ and $\beta(\Theta)$ are unknown functions of the material porosity Θ, $\sigma_z, \sigma_\varphi, \sigma_r$ are the stress tensor components.

It is assumed, that in the case of compacting the material in a closed chamber with smooth walls (with the friction omitted), at any height of compacting stamp position, the sample is homogeneous within the entire volume and its density depends solely on the instantaneous stamp position relative to the chamber bottom. The variations of the stresses σ_r and σ_z are the functions of the material porosity Θ [21]:

$$\sigma_r = \xi(\Theta)\sigma_z, \qquad (2)$$

where $\xi(\Theta) = [1 - 2\alpha(\Theta)]/[1 + 4\alpha(\Theta)]$ is the function defining the lateral pressure coefficient, and

$$\sigma_z \equiv \sigma_z(\Theta) = 3^{-1}\sqrt{[1 + 4\alpha(\Theta)]\beta(\Theta)/\alpha(\Theta)}\,\sigma_Y. \qquad (3)$$

The elementary Eq. (2) serves for determining the function $\alpha(\Theta)$, with the material friction against the chamber and stamp walls being eliminated. Such tests include the measurement of the force acting on the half-mould, originating from the lateral pressures and the force acting on the ram during material compaction. By determining this function it is possible to determine the porosity function $\beta(\Theta)$ and the value of the compressive yield strength σ_Y using Eq. (3).

Under actual compacting conditions the friction of the material against the mould walls occurs, which causes a non-uniform material density distribution and differences in axial stress magnitudes between the compacting stamp and the chamber bottom. It is assumed that friction forces occur only within the narrow zones adjacent to the chamber walls, whereas the friction on the stamp walls and the chamber bottom is omitted due to the absence of displacements in the radial direction; therefore the friction force work on those surfaces is equal to zero, thus having no effect on the compaction process. In that case the axial component of σ_z stress in the cross-section has a uniform distribution, therefore the distribution of pressures on the stamp and on the chamber bottom is also uniform.

Expression (3) that defines the σ_z stresses for frictionless compaction remains valid only for a certain cross-section $z < h$ with a density (or porosity) equal to the average material density (porosity). Based on the hypothesis of the linear distribution of thickened material density [22], it is assumed that the average (apparent) density is at the mid-height *h*.

From the condition of the balance of forces acting on an infinitely small material volume element of a thickness *dz*, and after making the necessary arrangement, the following has been obtained (Fig. 1):

$$d\sigma_z = 2\tau_n / R\, dz, \tag{4}$$

where $\tau_n = \tau_n(\Theta) = m_L(1-\Theta)^{2/3}\sqrt{\beta(\Theta)/3}\,\sigma_Y$ are the tangential stresses, m_L is the Prandtl friction coefficient of compact material [23], *R* is the chamber radius.

By integrating both sides of Eq. (4), while adopting the Prandtl friction model and assuming the linear distribution of density (or porosity) along the sample height, the following expression is obtained:

$$\int_{\sigma_z(\Theta_m)}^{\sigma_z} d\sigma_z = \int_{h/2}^{z} 2\tau_n / R\, dz \,. \tag{5}$$

After integration of equation (5) and making appropriate transformations we find:

$$\sigma_z(z) = \sigma_z(\Theta_m) + 2\tau_n(\Theta_m)[z - h/2]/R\,, \tag{6}$$

where Θ_m is the average sample porosity, described by the relationship:

$$\Theta_m = 1 - \rho_m/\rho_L = 1 - m_p/(\pi R^2 h \rho_L)\,,$$

where ρ_m is the average density of a sample of the height *h*, ρ_L is the density of the solid (compact) material of the porosity $\Theta = 0$, m_p is the sample mass.

Based on expression (6), the forces acting on the stamp, P^+ at $z = h$ and on the chamber bottom, P^- at $z = 0$, are as follows (Fig. 1):

$$P^{\pm} = \pi R^2[\sigma_z(\Theta_m) \pm \tau_n(\Theta_m)h/R]. \tag{7}$$

The magnitude of force P_b acting on the half-chamber, originating from the radial stresses is determined from the formula:

$$P_b = \int_0^h 2\xi(\Theta_m)\sigma_z(z)R dz\,, \tag{8}$$

After integration of the relationhip (8) we obtain:

$$P_b = 2\xi(\Theta_m)\sigma_z(\Theta_m)Rh\,. \tag{9}$$

In the case of Amontons–Coulomb type of friction $\tau_n = \mu\sigma_n$ equation (5) takes the form:

$$\int_{\sigma_z(\Theta_m)}^{\sigma_z} d\sigma_z/\sigma_z = 2\mu R^{-1}\int_{h/2}^{z} \xi(\Theta_m)\, dz\,, \tag{10}$$

where $\mu = \mu_L(1-\Theta_m)^{-2/3}$, μ_L is the Amontons–Coulomb friction coefficient of the compact material [23].

By solving equation (10) after some transformations, we find

$$\sigma_z(z) = \sigma_z(\Theta_m)\exp\{2\mu\xi(\Theta_m)[z - 0.5h]/R\}.$$

Finally, by proceeding similarly as for the Prandtl type friction, the following expressions is obtained:

$$\begin{aligned} P^{\pm} &= \pi R^2 \sigma_z(\Theta_m)\exp[\pm\mu\xi(\Theta_m)h/R], \\ P_b &= \mu^{-1}\exp[-h\xi(\Theta_m)\mu/R]\{\exp[2h\xi(\Theta_m)\mu/R] - 1\}\sigma_z(\Theta_m). \end{aligned} \tag{11}$$

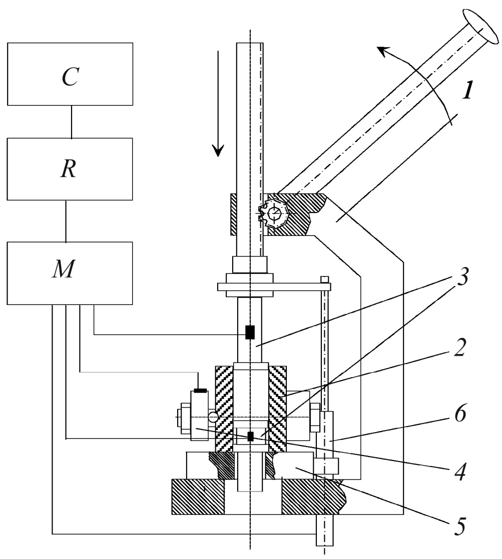

Fig. 2. Schematic diagram of the SJ-3 test stand: *1* – manual press; *2* – divided compaction chamber, *3* – upper and lower stamps (extensometric force transducers); *4* – clamping ring (an extensometric force transducer); *5* – base; *6* – TPP 100 transformer displacement transducer; *C* – computer; *M* – KWS/6a-5 extensometric bridge; *R* – MC201A recorder.

The test stand for the determination of the compound feed mechanical properties. To determine the material constants of the compound feed an SJ-3 test stand was built, whose schematic is illustrated in Fig. 2. The test stand includes small workshop press *1*, using which the compound feed poured to chamber *2* is thickened.

The compaction chamber has been split along the opening axis, and then fastened together with clamping ring *4* allowing the measurement of forces acting on the half-chamber (half-mould). The compaction of the compound takes place with the upper stamp, with the lower stamp constituting the constructional bottom of the chamber. Upper and lower stamps *3* are extensometric force transducers. In order to determine the sample density during compaction, a TPP 100 transformer displacement transducer was fixed to the lower base *5* and the upper stamp.

Signals from the stamps, the clamping ring and the displacement transducer were routed to the KWS/6a-5 extensometric bridge and then connected to the MC201A recorder coupled with a notebook computer. For recording measurements, the MC201.EXE program was employed, whereby the measurements were stored on the hard disk in the form of binary files. The stored files were subjected to further analysis using the authors own software.

The measurement of the compaction forces on the upper and lower stamps enabled the determination of the friction forces occurring between the material being compacted and the mould walls. The friction force is the difference between the force occurring on the upper stamp and the force on the lower force.

Identification of the material parameters. During measurements, strong adhesion of the compound feed to the mould walls was noticed to exist for testing temperatures from 40 to 90°C. This decided the use of the Prandtl friction model for identification in this temperature range. In the case of the temperature of 10°C, no adhesion of the compound feed to the mould walls occurred, therefore at this temperature the Amontons–Coulomb friction model was employed.

As the porosity function form the Shima-Oyane functions were adopted [16]:

$$\alpha(\Theta) = D\Theta^E, \qquad \beta(\Theta) = (1-\Theta)^C, \tag{12}$$

where C, D, E are the parameters of the porosity function.

The recorded experimental points of forces acting on the lower stamp, upper stamp and half-mould during compaction were approximated by the least squares method by minimizing the following expression:

$$\sum_{i=n_p}^{n_k} \left[(P_i^+ - P_i^{+'})^2 + (P_i^- - P_i^{-'})^2 + (P_{ib} - P_{ib}^{'})^2 \right]. \tag{13}$$

where P_i^+, P_i^-, P_{ib} is the i-th points of the function of the approximated force on the upper stamp, lower stamp and mould clamp, $P_i^{+'}, P_i^{-'}, P_{ib}^{'}$ is the i-th points of the recorded force on the upper stamp, lower stamp and mould clamp. The minimization of expression (13) was made within the measurement point range from n_p (defined for the material bulk density of ρ_u = 570 kg/m^3) to n_k (defined for the upper stamp force corresponding to the unit compaction pressures of 50 MPa).

This method enables all parameters being identified to be obtained in a single search, while considering the recorded curves of forces on the upper stamp, lower stamp and mould clamp. In the case of the lateral force measurement curve, the approximation considered points lying above the force corresponding to the clamping ring pre-tension.

In the case of using the Prandtl friction model, equations (7) and (9) were used in identification, while for the Amontons–Coulomb model, equations (11). As the solid material density, ρ_L, the density of the material compacted in the closed chamber at a pressure of 200MPa was adopted for the compound at varying temperature. No significant changes in this density were observed during measurements. The average of 12 measurements being equal to ρ_L = 1498 kg/m^3 was assumed.

The approximation was made with respect to the values of C, D, E, σ_Y, m_L (μ_L). For searching the minimum of the square sum function, the Hook-Jeeves simple search gradientless method was used. Then, the average values obtained for each temperature were approximated with either an exponential or linear function. Due to the small changes in C, D porosity function values, the average values were assumed for the entire temperature variation interval. Because of the friction law change at the temperature of 10°C, the variations in the Prandtl friction coefficient m_L were approximated from 40°C.

Examples of graphical identification results obtained based on the experimental data together with the model curves are shown in Fig. 3.

In the identification carried out, the R^2 squared regression coefficient values above 99% were obtained, which indicates good consistence between the experimental and the model curves. The achieved consistence provides an evidence for the possibility of using the metal powder theory of plasticity for the study of compound feed agglomeration processes.

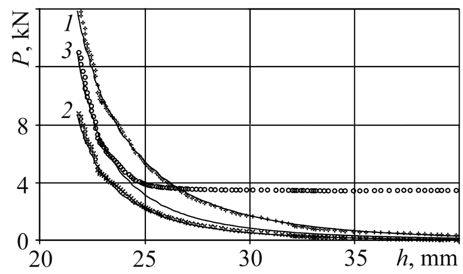

Fig. 3. Example of diagrams of the variations of forces P^+ (curve *1*); P^- (curve *2*); P_b (curve *3*), together with the model curves (T = 40°C) using the Prandtl friction model.

In the case of using the Prandtl friction for the temperature of 10°C and the Amontons–Coulomb friction (the underlined value) for temperatures above 40°C, greater discrepancies between the experimental curves and the model curves and the lower R^2

regression coefficient values were obtained. The obtained average values of individual compound feed material parameters at the temperatures examined are given in Table.

Average values of the identified compound feed parameters

Test temperature T, °C	Yield strength σ_Y, MPa	Friction coefficient $m_L(\mu_L)$	Porosity function (12) parameters		
			C	D	E
10	37,74	0,1227	12,19	0,2204	0,3744
40	25,80	0,3686	12,12	0,2428	0,5089
53	20,70	0,3398	12,25	0,1981	0,5948
65	17,13	0,2677	12,25	0,2210	0,7386
78	13,94	0,2372	12,48	0,2297	0,8341
90	14,59	0,1949	12,05	0,2562	0,9738

The obtained results of approximation of the average material parameters shown in Table 1. as a function of temperature are represented by the formulae: $\sigma_Y = 43.16\times\exp(-0.0135T)$; $E = 0.3178\exp(0.01243T)$; $C = 12.22$; $D = 0.228$ for 10°C < T < 90°C and Prandtl friction coefficient $m_L = -0.003594T + 0.516$ at 40°C < T < 90°C.

CONCLUSIONS

The investigation of the closed-chamber pressure agglomeration process enables the determination by the identification method of basic material parameters, such as: settling density, maximum density and the shear yield strength. It is established, that: the consistence between the behaviour of the experimental and the theoretical stamp compaction pressure variations curves provides an evidence for the correctness of the assumed density-reinforcement ideally plastic loose body model and the yield criterion used in mathematical modelling of the closed-chamber compound feed compaction process; the results of this examination can be used for modelling other, more complex processes of compound feed pressure agglomeration in granulating machines.

For the description of the stress and strain state in the processes of compacting plant materials with plastic features, aside from the thin cross-section method, also more advanced methods, such as the characteristics method or MES, can be used.

РЕЗЮМЕ. Отримано формули для розрахунку напружень і деформацій під час ущільнення матеріалів рослинного походження. Математична модель цього процесу ґрунтується на умові пластичності Ґріна з використанням функції поруватості, а також законів тертя Кулона–Амонтона і Прандтля для поруватих матеріалів. Числовий аналіз і його експериментальну верифікацію виконано для ущільнення рослинної суміші в закритій камері. Необхідні для цього механічні сталі матеріалу ідентифіковано за допомогою числових методів і рівнянь нелінійної регресії, що описують тиск на преси.

РЕЗЮМЕ. Получены формулы для расчета напряжений и деформаций при уплотнении материалов растительного происхождения. Математическая модель этого процесса базируется на условии пластичности Грина с использованием функции пористости, а также законов трения Кулона–Амонтона и Прандтля для пористых материалов. Численный анализ и его экспериментальную верификацию выполнено для уплотнения растительной смеси в закрытой камере. Необходимые для этого механические постоянные материала идентифицировано с помощью численных методов и уравнений нелинейной регрессии, описывающих давление на прессы.

1. *German R. M.* Powder Metallurgy and Particulate Materials Processing // Metal Powder Industries Federation. – New Jersey: Princeton, 2005. – 528 p.

2. *Youseffi M. and Showaiterv N.* PM Processing of elemental and pre-alloyed 6061 aluminum alloy with and without common lubricants and sintering aids // Powder Metallurgy. – 2006. – **49**, № 3. – P. 240–252.
3. *Volger T. J., Lee M. Y., and Grady D. E.* Static and dynamic compaction of ceramic powders // Int. J. Sol. Struct. – 2007. – **44**, № 2. – P. 636–658.
4. *Wing Z. N. and Halloran J. W.* Dry Powder Deposition and Compaction for Functionally Graded Ceramics // J. Am. Cer. Soc. – 2006. – **89**, № 11. – P. 3406–3412.
5. *Narayan P. and Hancock B. C.* The influence of particle size on the surface roughness of pharmaceutical compacts // Mat. Sci. and Eng. A. – 2005. – **407**, № 1. – P. 226–233.
6. *Modeling* the mechanical behaviour of pharmaceutical powders during compaction / C. Y. Wu, O. M. Ruddy, A. C. Bentham, B. C. Hancock, S. M. Best, and J. A. Elliott // Powder Techn. – 2005. – **152**, № 1–3. – P. 107–117.
7. *Laskowski, J.* Studia nad procesem granulowania mieszanek paszowych. – Lublin: Wydawnictwo Akademii Rolniczej, 1989. – 113 s.
8. *Chou C. S., Sheau-Horng Lin S. H., and Wen-Chung Lu W. C.* Preparation and characterization of solid biomass fuel made from rice straw and rice bran // Fuel Proc. Tech. – 2009. – **90**, № 7–8. – P. 980–987.
9. *Mediavilla I., Fernández M. J., and Esteban L. S.* Optimization of pelletisation and combustion in a boiler of 17.5kWth for vine shoots and industrial cork residua // Fuel Proc. Tech. – 2009. – **90**, № 4. – P. 621–628.
10. *Chen W. F. and Saleeb A. F.* Constitutive equations for engineering materials. Elasticity and modeling. – New York: Wiley Inter-science, 1982. – **Vol. 1.** – 580 p.
11. *Drucker D. C. and Prager W.* Soil mechanics and plastic analysis on limit design // Q. Appl. Math. – 1952. – **10**, № 2. – P. 157–165.
12. *Schofield A. N. and Wroth C. P.* Critical State Solid Mechanics. – London: McGraw–Hill, 1968. – 218 p.
13. *Lade P. V.* Elastic–plastic stress–strain theory for cohesion less soil with curved yield surfaces // Int. J. Solids and Struct. – 1977. – **13**, № 11. – P. 1019–1035.
14. *Green R. J.* A plasticity theory for porous solids // Int. J. Mech. Sci. – 1972. – **14**, № 4. – P. 215–224.
15. *Kuhn H. A. and Downey C. L.* Deformation characteristics and plasticity theory of sintered powder materials // Int. J. Powder Metallurgy. – 1971. – 7, № 1. – P. 15–25.
16. *Shima S. and Oyane M.* Plasticity theory for porous metals // Int. J. Mech. Sci. – 1976. – **18**, № 6 – P. 285–291.
17. *Doraivelu M.* A new yield function for compressible P/M materials // Int. J. Mech. Sci. – 1984. – **26**, № 9–10. – P. 527–535.
18. *Gurson A. L.* Continuum theory of ductile rupture by void nucleation and growth; I. Yield criteria and flow rules for porous ductile media // J. Eng. Mater. Tech. –1977. – **99**, № 1. – P. 2–15.
19. *Czaban J. and Kamiński Z.* Theoretical foundations of compaction and compression of granular materials of vegetable origin with properties of plasticity // Acta Agrophysica. – 2012. – **19**, № 3. – P. 487–500.
20. *Die* compaction of copper powder designed for material parameter identification / W. Bier, M. P. Dariel, N. Frage, S. Hartmann, and O. Michailov // Int. J. Mech. Sci. – 2007. – **49**, № 7. – P. 766–777.
21. *Okoński St.* Podstawy plastycznego kształtowania materiałów spiekanych z proszków metali. – Krakow: Wydawnictwa Politechniki Krakowskiej, 1993. – 203 s.
22. *Лаптев А. М.* Анализ формования и допрессовки пористых втулок методом тонких сечений // Порошковая металлургия. – 1988. – № 7. – С. 44–48.
23. *Друянов Б. А.* Прикладная теория пластичности пористых тел. – М.: Машиностроение, 1989. – 168 с.

Received 10.11.2015